ELSEVIER

Biochimica et Biophysica Acta 1463 (2000) 323–332

BIOCHIMICA ET BIOPHYSICA ACTA
BBA

www.elsevier.com/locate/bba

Deuterium NMR investigation of an amphotericin B derivative in mechanically aligned lipid bilayers

Andrew W. Hing [a], Jacob Schaefer [a,*], George S. Kobayashi [b]

[a] *Department of Chemistry, Washington University, St. Louis, MO 63130, USA*
[b] *Division of Infectious Diseases and Division of Laboratory Medicine, Washington University School of Medicine, St. Louis, MO 63110, USA*

Received 6 July 1999; received in revised form 24 October 1999; accepted 28 October 1999

Abstract

The methyl-d_3 amide derivative of the polyene antibiotic amphotericin B was synthesized, assayed for biological activity, incorporated into mechanically aligned bilayers of dipalmitoylphosphatidylcholine (DPPC), and examined by deuterium and phosphorus NMR. The amide derivative has a lesser, but qualitatively similar, biological activity relative to amphotericin B. Incorporation of the amide derivative and ergosterol into aligned DPPC bilayers resulted in a single, stable bilayer phase, as shown by phosphorus NMR of the DPPC headgroups. Deuterium NMR spectra revealed one major ^2H quadrupolar splitting and one major ^2H–^1H dipolar splitting in the liquid-crystalline phase, consistent with a high degree of alignment and a single, averaged physical state for amphotericin B methyl-d_3 amide in the bilayer. Variations of the quadrupolar and dipolar splittings as a function of macroscopic sample orientation and temperature indicated that the amide derivative undergoes fast rotation about a motional axis that is parallel to the bilayer normal.

Keywords: Amphotericin B derivative; NMR; Lipid bilayer

1. Introduction

With increased use of immunosuppressive therapies as part of organ transplantation and the advent of immunocompromising diseases such as AIDS, fungal disease has assumed greater importance in the clinical management of already compromised patients. For treatment of systemic fungal infections, amphotericin B is still considered the gold standard. Unfortunately, amphotericin B is not a benign drug and possesses severe side effects. Efforts to improve the therapeutic profile of the drug have included chemical derivatization [1–3] and alterations in the mode of drug delivery [4,5].

Prevailing models of the mechanism of action of amphotericin B postulate formation of ion-permeable membrane channels as the direct cause of amphotericin B activity and toxicity [6–8]. These channels result in selective permeability changes and subsequent cell death. Evidence that amphotericin B forms ion channels in membranes is provided by

Abbreviations: DPPC, dipalmitoylphosphatidylcholine; NMR, nuclear magnetic resonance; ESR, electron spin resonance; MIC, minimum inhibitory concentration; EFG, electric field gradient; t_R, recycle delay

* Corresponding author. Fax: +1-314-935-4481; E-mail: schaefer@wuchem.wustl.edu

0005-2736/00/$ – see front matter
PII: S0005-2736(99)00223-0

functional studies of ion conductance [9–12]. Because of the sterol dependence of channel formation, the selectivity of amphotericin B is thought to be due to a greater binding affinity for ergosterol in fungal membranes than for cholesterol in mammalian membranes [13,14]. However, this difference in binding affinity is not great and presumably results in the narrow range observed clinically between therapeutic and toxic levels.

Structurally, amphotericin B belongs to a class of molecules called polyenes which are characterized by the presence of a large lactone ring containing multiple, conjugated double bonds. An X-ray diffraction study of amphotericin has elucidated the overall structure of amphotericin B [15,16]. Insights into the structural organization of amphotericin B in membranes have been provided by various physical studies. Fluorescence and magnetic resonance studies have been used to study membrane-bound polyene antibiotics indirectly, through their effects on appropriately labeled sterols, phospholipids, or other membrane probes [17–23]. In contrast, circular dichroism provides a direct method for monitoring amphotericin B in membranes. Studies based on this technique indicate the presence of multiple polyene species and provide information about their relative amounts [12,24–26]. Another technique, polarized absorption spectroscopy, has yielded information about amphotericin B orientation in lipid monolayers [27]. In a study based on electron spin resonance, ESR spectra showed that a spin-labeled derivative of amphotericin B in lipid vesicles possessed a high degree of motion and was not aggregated [28].

The use of solid-state NMR techniques allows amphotericin B to be studied in a physiologically relevant environment at atomic resolution. However, introducing a stable-isotope label into amphotericin B by chemical synthesis is difficult [29–31]. Perhaps, a more cost-effective, initial strategy is to introduce a stable-isotope label by chemical modification and to study the resulting amphotericin B derivative. Such a derivative can be expected to provide insights into amphotericin B behavior based on the similarity between semi-synthetic derivatives and amphotericin B in their mode of action [32–35].

In this study, a methyl-d_3 amide derivative of amphotericin B was synthesized and incorporated into mechanically aligned DPPC bilayers. Phosphorus NMR spectra of the phosphocholine headgroup of DPPC provided information about the behavior of the surrounding bilayer while deuterium NMR spectra of the deuterated methyl group allowed the orientation and motion of the derivative to be monitored. The resulting data show that amphotericin B methyl-d_3 amide is uniformly aligned in a membrane environment and undergoes fast rotation about an axis that is parallel to the bilayer normal.

2. Materials and methods

2.1. Amphotericin B methyl-d_3 amide synthesis

The methyl-d_3 amide of amphotericin B was synthesized by the azide method and purified by countercurrent distribution according to a general procedure described in the literature [3]. In particular, 138 mg of amphotercin B (E.R. Squibb and Sons, Princeton, NJ) was reacted with 210 mg of methyl-d_3-amine hydrochloride (98+atom % D, Aldrich, Milwaukee, WI) in 18.0 ml dimethylformamide using 0.65 ml of diphenylphosphoryl azide and 1.00 ml of triethylamine. Subsequent countercurrent distribution was performed with chloroform–methanol–water in a volume ratio of 2:2:1. Fast-atom bombardment mass spectrometry showed ions consistent with the molecular weight (940) and primary structure of the desired product. Thin-layer chromatography showed only one spot corresponding to the desired product; no unreacted amphotericin B was detected.

2.2. Amphotericin B methyl-d_3 amide activity

2.2.1. Potassium leakage

Polyene-induced potassium leakage from *Candida albicans* and human erythrocytes was measured according to a previously described procedure (Kotler-Brajtburg et al., [32]). Cells of *C. albicans* B311 used in the measurements were obtained from our stock culture collection and maintained on Sabouraud dextrose agar slants. Appropriately prepared samples of fungal cells or erythrocytes were incubated with varying concentrations of either amphotericin B methyl-d_3 amide or a corresponding amount of amphotericin B as Fungizone (Bristol-Myers Squibb,

Princeton, NJ). The results were calculated and expressed as a percentage of the control samples. From a graphic plot of the data, the concentration of antibiotic required for a 50% effect was calculated.

2.2.2. Minimum inhibitory concentration (MIC)

The MIC was considered to be the lowest concentration of amphotericin B methyl-d_3 amide or amphotericin B (Fungizone) that completely inhibited growth of *C. albicans* B311 cells.

2.3. Membrane incorporation

A previously developed protocol for preparation of aligned bilayers [36] proved sufficiently robust that the same methodology could be used to incorporate the polyene derivative into sterol-containing DPPC bilayers. In this protocol, inclusion of water in the deposition solvent plays a critical role in the alignment process. In the present study, amphotericin B methyl-d_3 amide, ergosterol (Sigma), and DPPC (Avanti) were dissolved in a solution of 94.9% methanol in deuterium-depleted water (Isotec) before deposition onto glass coverslips and subsequent hydration. Based on the weight of materials used, the NMR sample contained a total of 2.5 mg of the material produced by derivatization of amphotericin B, and the polyene:sterol:phospholipid molar ratios were estimated to be $\sim$1:2:100.

2.4. NMR data acquisition

2.4.1. NMR instrumentation

NMR data were acquired using a transmission-line probe tuned to the ^{1}H, ^{31}P, and ^{2}H Larmor frequencies of 300, 121, and 46 MHz, respectively, and a Chemagnetics/Varian CMX300 spectrometer (Fort Collins, CO) equipped with PTS 500 and PTS 160 frequency synthesizers (Programmed Test Sources, Acton, MA). Power amplifiers included models 166UP and LP1000 (Kalmus Engineering International, Woodinville, WA) operating at ^{1}H and ^{31}P Larmor frequencies, respectively; and an LPI-10 model (ENI Power Systems, Rochester, NY) operating at the ^{2}H Larmor frequency.

2.4.2. ^{31}P-NMR acquisition parameters

All phosphorus spectra were acquired with a single, phase-cycled, 30-μs pulse. A spectral width of 40 kHz was used to collect the 4096 points constituting each spectrum, resulting in a digital resolution of 9.766 Hz/point. Proton decoupling was applied with a duty cycle of 0.3%. In each plot, zero ppm represents the resonance frequency of external 85% phosphoric acid.

2.4.3. ^{2}H-NMR acquisition parameters

All deuterium spectra were acquired with a phase-cycled, composite (form II) quadrupole echo sequence [37]. The 90° pulse width was 5 μs, and the interpulse delay was 30 μs. A spectral width of 100 kHz was used to collect 16384 points for each spectrum, yielding a digital resolution of 6.104 Hz/point. The duty cycle of applied proton decoupling was 0.8%. In each plot, zero Hz represents the resonance frequency of external ^2H_2O.

2.4.4. Temperature regulation

Temperature control was provided by an XRII851 Air-Jet Crystal Cooler equipped with a TC-84 temperature controller and an AD-80 air dryer (FTS Systems, Stone Ridge, NY). A thermocouple (Omega Engineering, Stamford, CT) was used to monitor the temperature of the air at the exhaust port of the probe head. The sample was allowed to equilibrate at each temperature T for at least 0.5 h prior to data acquisition. The transition between sample temperatures was accomplished by changing T by 10°C over a period of $\geq$0.5 h (unless otherwise noted).

2.4.5. Macroscopic sample orientation

The orientation of the sample in the magnetic field was quantified by the angle β between the normal to the glass coverslips and the direction of the magnetic field. Data were acquired at two different macroscopic sample orientations: $\beta=0°$ and $\beta=90°$.

2.4.6. Sample stability

All NMR signals were stable over the time periods required to acquire spectra. Furthermore, preparation of similar, aligned bilayer samples from different synthetic batches of amphotericin B methyl-d_3 amide confirmed the reproducibility of the acquired data.

3. Results

3.1. Chemical structure of amphotericin B methyl-d_3 amide

Fig. 1 shows the chemical structure of amphotericin B methyl-d_3 amide. The amide bond between C-41 and the amide nitrogen is assumed to form with the methyl-d_3 group trans to the macrolide ring so that the two bulkiest substitutents are furthest from each other. Moreover, because crystal structures of typical methyl amide compounds show their coordinates to be in good agreement with those of the *trans* peptide bond [38], the backbone atoms in the methyl-d_3 amide group of the derivative can be viewed as forming a peptide plane.

The mycosamine sugar moiety and the macrolide lactone ring of the parent amphotericin B compound remain unaltered. In particular, the macrolide ring retains the rigidity conferred by the ketal ring and the fully extended, *trans*-configured, conjugated double bonds [16]. A quantitative representation of the entire amphotericin B methyl-d_3 amide molecule is obtained by constructing a methyl-d_3 amide plane based on the coordinates of a peptide plane [39] and then grafting the methyl-d_3 amide plane onto the X-ray coordinates that represent amphotericin B [16]. A single, direct bond denoted by C-16–C-41 connects the methyl-d_3 amide group to the rest of the

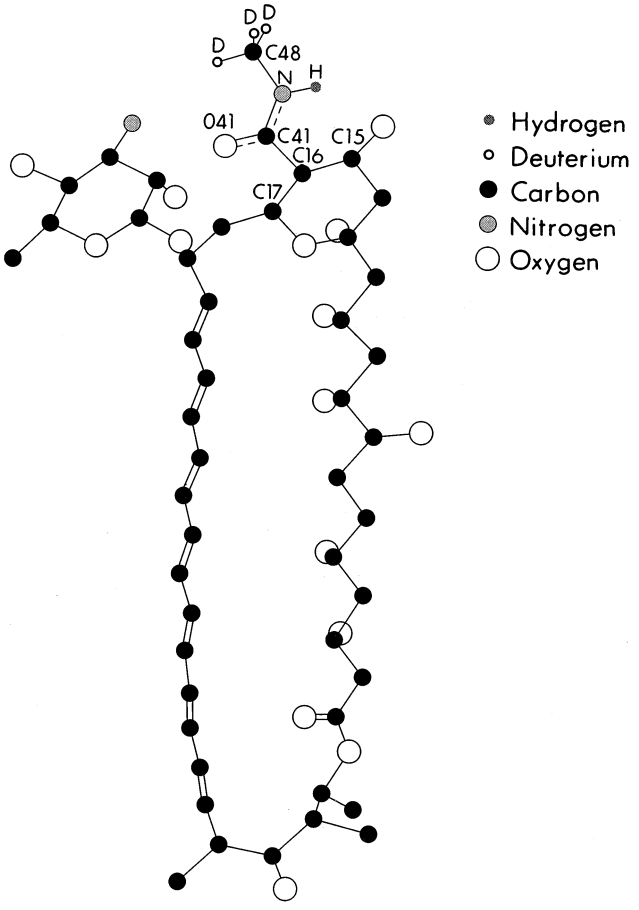

Fig. 1. Chemical structure of amphotericin B methyl-d_3 amide.

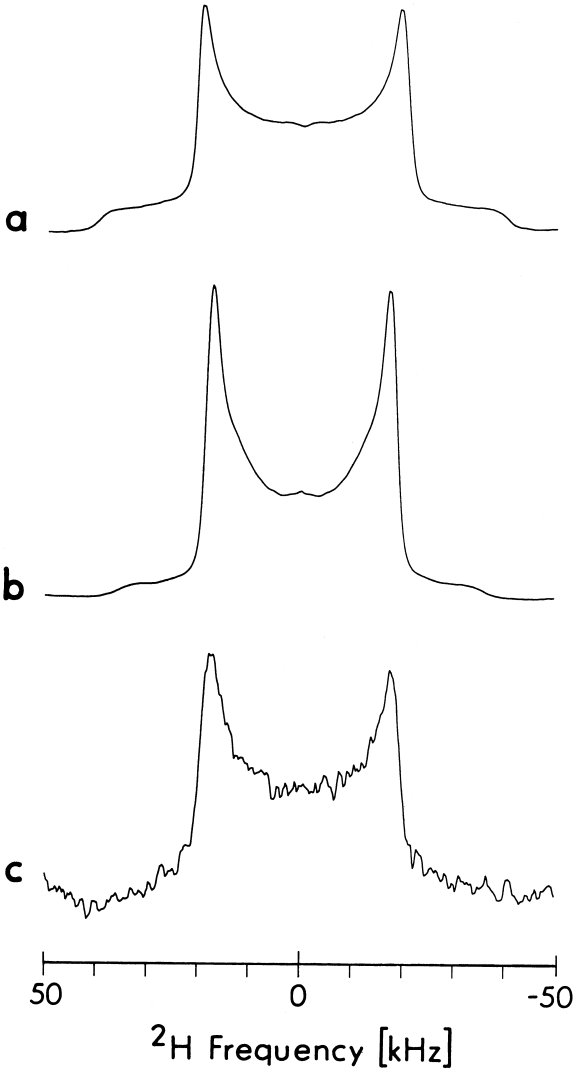

Fig. 2. ^{2}H-NMR spectra of the powder form of: (a) 100 mg of L-[3,3,3-d_3]alanine acquired at $T = 4$°C with $t_R = 1.0$ s and 3072 scans; (b) 100 mg of methyl-d_3-amine hydrochloride acquired at $T = -39$°C with $t_R = 16.0$ s and 2560 scans; and (c) 7 mg of amphotericin B methyl-d_3 amide acquired at $T = -40$°C with $t_R = 16.0$ s and 81904 scans. The spectra were acquired without ^{1}H decoupling and are plotted with 500 Hz of line broadening.

amphotericin B derivative (Fig. 1). The molecule possesses a degree of freedom arising from rotation about the C-16–C-41 bond axis. However, rotation about this axis has only a minor effect in decoupling the methyl-d_3 quadrupolar splitting from the overall behavior of the entire molecule because the C-16–C-41 bond and the N_{amide}-C-48 bond are roughly parallel, differing in orientation by only 9°.

3.2. Activity of amphotericin B methyl-d_3 amide

For induction of 50% leakage of potassium from *C. albicans* B311, the required concentration of powder containing amphotericin B methyl-d_3 amide was approximately 1–3 times greater than that of amphotericin B as Fungizone. On the other hand, for induction of 50% leakage of potassium from human erythrocytes, the required concentration of derivative-containing powder was approximately 5–6 times greater than that of amphotericin B. In addition, the MIC of product containing amphotericin B methyl-d_3 amide was measured to be 3.125 μg/ml while that of amphotericin B as Fungizone was 0.391 μg/ml. These data show that the biological activity of the methyl-d_3 amide derivative relative to amphotericin B is consistent with the activities exhibited by other amide derivatives of amphotericin B [3,40–42]. Most importantly, these results provide an indication that amphotericin B methyl-d_3 amide functions in a qualitatively similar manner to amphotericin B, but is about 8-fold less potent.

3.3. Powder form of amphotericin B methyl-d_3 amide

Deuterium NMR spectra of two common reference compounds and amphotericin B methyl-d_3 in

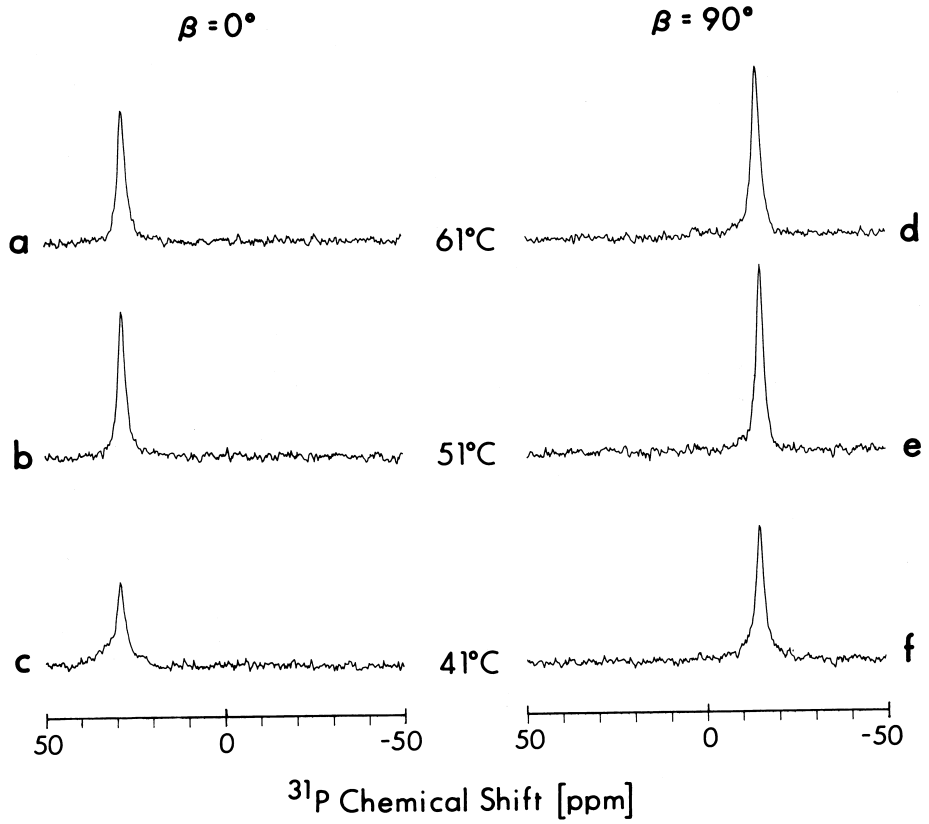

Fig. 3. ^{31}P-NMR spectra of DPPC bilayers containing amphotericin B methyl-d_3 amide and ergosterol acquired at temperatures $T = 61$°C (a,d), 51°C (b,e), and 41°C (c,f), and sample orientations $\beta = 0$° (a-c) and $\beta = 90$° (d–f). The full-width at half-maximum intensity of individual peaks is 2–3 ppm. Spectra were acquired with $t_R = 8.0$ s, 292 scans, and 10-kHz ^{1}H decoupling, and are plotted with 30 Hz of line broadening.

Table 1
^{31}P-NMR chemical shift anisotropy of aligned DPPC bilayers containing amphotericin B methyl-d_3 amide and ergosterol as a function of temperature and sample orientation

T (°C)	ν_{CSA} (ppm)	
	$\beta = 0°$	$\beta = 90°$
61	28.0	−14.5
51	28.3	−15.1
41	28.8	−15.0

powder form are shown in Fig. 2. The spectra represent typical Pake patterns generated by randomly oriented, quadrupolar interactions. Due to methyl rotational averaging of the C–D EFG about the C_3 symmetry axis, the effective EFG tensor is axially symmetric with the unique principal axis along the C_3 symmetry axis. The symmetry axis is the C_α–C_β bond in L-[3,3,3-d_3]alanine (Fig. 2a), the N–C bond in methyl-d_3-amine hydrochloride (Fig. 2b), and the N_{amide}–C-48 bond in amphotericin B methyl-d_3 amide (Fig. 2c). The peak-to-peak splittings measured at half-maximum intensity without added line broadening are 41.3 kHz (Fig. 2a), 37.5 kHz (Fig. 2b), and 39.7 kHz (Fig. 2c). The widths of the peak-to-peak splittings correspond to the quantity $|(1/4)(e^2qQ/h)|$ for typical methyl-d_3 rotation, where e^2qQ/h is the static quadrupolar coupling constant.

3.4. Liquid-crystalline phase of the bilayer sample

3.4.1. DPPC

Phosphorus NMR spectra of the phospholipid/sterol/polyene sample in the liquid-crystalline phase are shown in Fig. 3. The single peak in each spectrum arises from the phospholipid headgroups and reflects the presence of a single lipid phase. The narrow line width of each peak proves that all DPPC

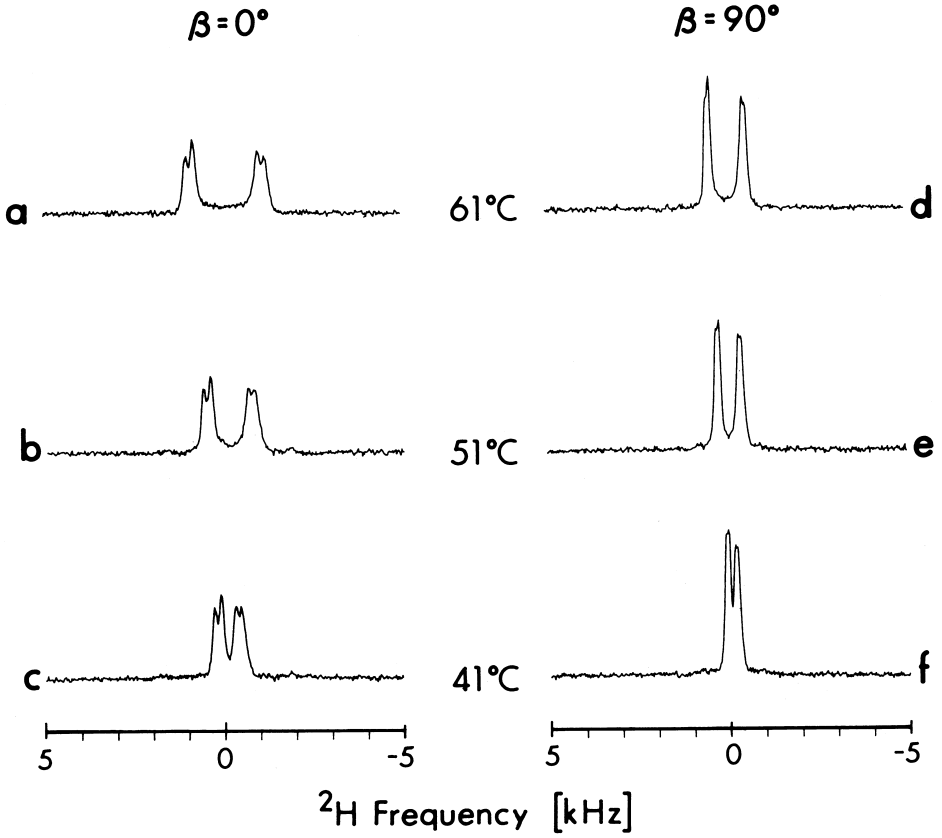

Fig. 4. ^{2}H-NMR spectra of amphotericin B methyl-d_3 amide in ergosterol-containing DPPC bilayers acquired at temperatures $T = 61$°C (a,d), 51°C (b,e), and 41°C (c,f), and sample orientations $\beta = 0°$ (a–c) and $\beta = 90°$ (d–f). No peaks are present outside the plotted frequency range. Spectra were acquired with $t_R = 0.5$ s, 49152 scans, and no ^{1}H decoupling, and are plotted with 10 Hz of line broadening.

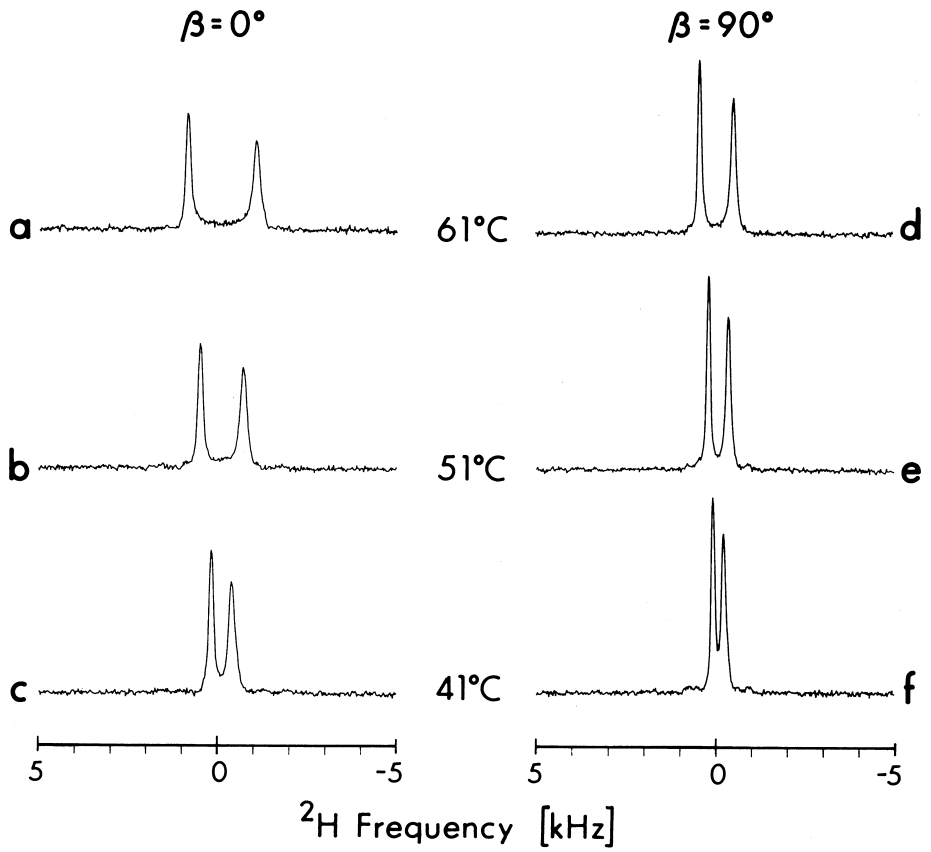

Fig. 5. Proton-decoupled ^{2}H-NMR spectra of amphotericin B methyl-d_3 amide in ergosterol-containing DPPC bilayers acquired at temperatures $T = 61$°C (a,d), 51°C (b,e), and 41°C (c,f), and sample orientations $\beta = 0°$ (a–c) and $\beta = 90°$ (d–f). The full-width at half-maximum intensity of individual peaks is on the order of 100–200 Hz. Spectra were acquired with $t_R = 0.5$ s, 49152 scans, and 3-kHz ^{1}H decoupling, and are plotted with 10 Hz of line broadening.

molecules have the same orientation. The chemical shift (ν_{CSA}) measured at $\beta = 0°$ is nearly twice that at $\beta = 90°$ (Fig. 3, Table 1), which indicates that DPPC headgroups rotate rapidly about a motional axis which is parallel to the coverslip normal [43]. This axis is also parallel to the bilayer normal because the coverslip and bilayer normals coincide in the liquid-crystalline phase. Identification of the long axis of the phospholipid as the motional axis is an arrangement that is consistent with the known structure of DPPC in liquid-crystalline bilayers [44,45].

The spectra in Fig. 3c and f were obtained at the nominal phase transition temperature of pure DPPC, $T = 41$°C. These spectra show that the majority of the sample remains liquid-crystalline. However, the broadening at the base of the peaks and concomitant decrease in peak heights reveal the presence of some gel-phase lipid and so indicate the onset of the phase transition.

3.4.2. *Amphotericin B methyl-d_3 amide*

Deuterium NMR spectra of the phospholipid/sterol/polyene sample in the liquid-crystalline phase have well-defined splittings and narrow line widths (Fig. 4), indicating a high degree of alignment. Each spectrum in Fig. 4 shows a major splitting of a few kHz with superimposed minor splittings of a few hundred Hz. The major splitting is the quadrupolar splitting of the methyl deuterons. The minor splittings disappear with proton decoupling (Fig. 5), and therefore are assigned to the dipolar interaction between the methyl deuterons and the adjacent single proton.

The presence of only a single quadrupolar splitting ($\Delta\nu_Q$) and a single dipolar splitting ($\Delta\nu_D$) shows that the methyl-d_3 amide group of the derivative adopts a single, average orientation in the lipid matrix. These splittings depend on the macroscopic sample orientation β (Fig. 4, Table 2). For the quadrupolar splitting, the equation describing rapid rotation of the

effective EFG tensor about a motional axis [46] becomes for a typical methyl rotor,

$$\Delta\nu_Q = (-1/2)(e^2qQ/h)\langle(3\cos^2\theta - 1)/2\rangle \times (3\cos^2\beta' - 1)/2 \quad (1)$$

The symbol θ represents the angle between the N_{amide}–C-48 bond and the motional axis; β' is the angle between the motional axis and the direction of the magnetic field; and $\langle\rangle$ denotes a time average over motions occurring during the time scale of the NMR measurement. The quadrupolar splittings measured at $\beta = 0°$ are twice those measured at $\beta = 90°$ (Table 2), which, according to Eq. (1), means that the quadrupolar tensor must rotate rapidly about a motional axis which is parallel to the coverslip (bilayer) normal so that $\beta' = \beta$. A similar analysis of the dipolar splittings yields the same conclusion. (Because of the rigid geometry of the backbone atoms of the methyl-d_3 amide group, the quadrupolar and dipolar splittings provide information about the same structural unit.)

The values of the splittings $|\Delta\nu_Q|$ and $|\Delta\nu_D|$ decrease as the temperature decreases (Figs. 4 and 5), with the change in $|\Delta\nu_D|$ much less than the change in $|\Delta\nu_Q|$. These trends are inconsistent with temperature-dependent motional averaging but can be attributed to slight changes in the bilayer orientation of the methyl-d_3 amide group with temperature. Such a change for the methyl-d_3 amide group will alter the orientations of quadrupolar and dipolar tensors differently with respect to the static field and hence result in different temperature trends for $|\Delta\nu_Q|$ and $|\Delta\nu_D|$. The integrated spectral intensity of the major peaks remains unchanged as a function of temperature, so the number of amphotericin B methyl-d_3 amide molecules contributing signal intensity to the major peaks remains constant.

Table 2
^{2}H-NMR quadrupolar splittings and ^{2}H–^{1}H dipolar splittings of amphotericin B methyl-d_3 amide in ergosterol-containing, aligned DPPC bilayers as a function of temperature and sample orientation

T (°C)	$\lvert\Delta\nu_Q\rvert$ (Hz)		$\lvert\Delta\nu_D\rvert$[a] (Hz)	
	$\beta = 0°$	$\beta = 90°$	$\beta = 0°$	$\beta = 90°$[b]
61	2000	1000	200	90
51	1240	620	180	80
41	560	240	160	70[c]

[a]The statistical significance of the slight differences between values of $|\Delta\nu_D|$ measured at different temperatures has not been determined.
[b]These values are estimates based on an analysis of spectral line shape.
[c]This value was confirmed by direct measurement of $|\Delta\nu_D|$ from a higher-quality spectrum obtained under identical conditions.

4. Discussion

4.1. Phospholipid phase behavior

The phosphorus NMR results show that the physical behavior of DPPC in the phospholipid/sterol/polyene sample is generally the same as that of pure DPPC. In the liquid-crystalline and gel phase of this sample, DPPC behaves similarly to pure DPPC exhibiting axial rotation in a single phase [47]. The measured ^{31}P chemical shift anisotropies (Table 1) are also in good agreement with previous measurements of pure DPPC [47–50]. Thus, the concentration of ergosterol (or amphotericin B methyl-d_3 amide) in the sample does not appear to be sufficient to alter significantly DPPC headgroup behavior. Interpreting the observed phosphorus line shapes in terms of the axial rotation and lateral diffusion of a pure phospholipid is therefore appropriate [51].

The effect of ergosterol (and polyene) on the gel/liquid-crystalline phase transition is minimal. The onset of minor line broadening in the ^{31}P-NMR spectra acquired at $T = 41$°C (Fig. 3c,f) is consistent with a phase transition temperature that is not significantly altered from that of pure DPPC. Given the small amount of ergosterol present in the sample (1:50, ergosterol:DPPC), such a result should probably be expected, especially since an analogous sterol, cholesterol, at a similar concentration does not greatly perturb the thermotropic phase behavior of DPPC [52,53].

4.2. Structural characteristics of amphotericin B methyl-d_3 amide, and motion and alignment in the bilayer

Analysis of the deuterium NMR data is greatly facilitated by the structure of amphotericin B meth-

yl-d_3 amide, whose relatively rigid macrolide ring and methyl-d_3 amide plane limit the degrees of conformational freedom. Furthermore, because the methyl-d_3 amide group is connected by a single, direct bond (C-16–C-41) to the rest of the amphotericin B derivative, the conclusion that the methyl-d_3 amide group rotates rapidly about an axis parallel to the bilayer normal strongly suggests that the entire polyene molecule undergoes the same motion.

The highly uniform alignment of amphotericin B methyl-d_3 amide molecules achieved in the liquid-crystalline phase demonstrates the sensitivity of the polyene to the orienting effects of the lipid matrix. The small, resolvable dipolar splittings in the deuterium NMR spectra (dipolar splittings as small as 70 Hz are resolved in some cases) would undoubtedly have been obscured under alignments that are only slightly less uniform.

Because amphotericin B methyl-d_3 amide has biological activity qualitatively similar to that of amphotericin B, we believe that what we learn about the amide derivative in bilayers is relevant to the behavior of amphotericin B itself. Experiments with the amide derivative are in progress to probe the polyene concentration dependence of bilayer orientation, aggregation, and channel formation.

Acknowledgements

This work was supported by The National Foundation for Infectious Diseases (NFID)/Janssen Pharmaceutica John P. Utz Fellowship in Medical Mycology (A.W.H.), NIH Grant GM50455 (J.S.), NIH Grant HL-55960 (G.S.K.), and NATO Grant SA 5-2-05 (G.S.K.). Thanks to Sharon J. Travis for maintenance and operation of the HPLC apparatus; Dr. Fong Fu Hsu for acquisition and interpretation of mass spectra; Svetlana Elberg for measurement of polyene activity; and Robert A. McKay for aid in construction and optimization of the NMR probe.

References

[1] W. Mechlinski, C.P. Schaffner, J. Antibiot. 25 (1972) 256–258.
[2] T. Bruzzese, M. Cambieri, F. Recusani, J. Pharm. Sci. 64 (1975) 462–463.
[3] A. Jarzebski, L. Falkowski, E. Borowski, J. Antibiot. 35 (1982) 220–229.
[4] R.R.C. New, M.L. Chance, S. Heath, J. Antimicrob. Chemother. 8 (1981) 371–381.
[5] F.C. Szoka Jr., M. Tang, J. Liposome Res. 3 (1993) 363–375.
[6] J. Bolard, Biochim. Biophys. Acta 864 (1986) 257–304.
[7] J. Brajtburg, W.G. Powderly, G.S. Kobayashi, G. Medoff, Antimicrob. Agents Chemother. 34 (1990) 183–188.
[8] S.C. Hartsel, C. Hatch, W. Ayenew, J. Liposome Res. 3 (1993) 377–408.
[9] T.E. Andreoli, Ann. New York Acad. Sci. 235 (1974) 448–468.
[10] R.W. Holz, Ann. New York Acad. Sci. 235 (1974) 469–479.
[11] A. Marty, A. Finkelstein, J. Gen. Physiol. 65 (1975) 515–526.
[12] G. Fujii, J.-E. Chang, T. Coley, B. Steere, Biochemistry 36 (1997) 4959–4968.
[13] J.D. Readio, R. Bittman, Biochim. Biophys. Acta 685 (1982) 219–224.
[14] N.M. Witzke, R. Bittman, Biochemistry 23 (1984) 1668–1674.
[15] W. Mechlinski, C.P. Schaffner, P. Ganis, G. Avitabile, Tetrahedron Lett. 44 (1970) 3873–3876.
[16] P. Ganis, G. Avitabile, W. Mechlinski, C.P. Schaffner, J. Am. Chem. Soc. 93 (1971) 4560–4564.
[17] D.B. Archer, Biochem. Biophys. Res. Commun. 66 (1975) 195–201.
[18] D.B. Archer, Biochem. Biophys. Res. Commun. 66 (1975) 1088.
[19] K. Ohki, Y. Nozawa, S.-I. Ohnishi, Biochim. Biophys. Acta 554 (1979) 39–50.
[20] A.C. Oehlschlager, P. Laks, Can. J. Biochem. 58 (1980) 978–985.
[21] E.J. Dufourc, I.C.P. Smith, H.C. Jarrell, Biochim. Biophys. Acta 776 (1984) 317–329.
[22] N. Henry-Toulme, M. Seman, J. Bolard, Biochim. Biophys. Acta 982 (1989) 245–252.
[23] M.P. Haynes, P.L.-G. Chong, H.R. Buckley, R.A. Pieringer, Biochemistry 35 (1996) 7983–7992.
[24] J. Bolard, M. Seigneuret, G. Boudet, Biochim. Biophys. Acta 599 (1980) 280–293.
[25] A. Vertut-Croquin, J. Bolard, M. Chabbert, C. Gary-Bobo, Biochemistry 22 (1983) 2939–2944.
[26] A.R. Balakrishnan, K.R.K. Easwaran, Biochemistry 32 (1993) 4139–4144.
[27] N. Ockman, Biochim. Biophys. Acta 345 (1974) 263–282.
[28] J.A. Urbina, B.E. Cohen, E. Perozo, L. Cornivelli, Biochim. Biophys. Acta 897 (1987) 467–473.
[29] K.C. Nicolaou, R.A. Daines, J. Uenishi, W.S. Li, D.P. Papahatjis, T.K. Chakraborty, J. Am. Chem. Soc. 110 (1988) 4672–4685.
[30] K.C. Nicolaou, R.A. Daines, T.K. Chakraborty, Y. Ogawa, J. Am. Chem. Soc. 110 (1988) 4685–4696.

[31] K.C. Nicolaou, R.A. Daines, Y. Ogawa, T.K. Chakraborty, J. Am. Chem. Soc. 110 (1988) 4696–4705.
[32] J. Kotler-Brajtburg, G. Medoff, G.S. Kobayashi, S. Boggs, D. Schlessinger, R.C. Pandy, K.L. Rinehart Jr., Antimicrob. Agents Chemother. 15 (1979) 716–722.
[33] K.M. Kasumov, M.P. Borisova, L.N. Ermishkin, V.M. Potseluyev, A.Y. Silberstein, V.A. Vainshtein, Biochim. Biophys. Acta 551 (1979) 229–237.
[34] M. Cheron, B. Cybulska, J. Mazerski, J. Grzybowska, A. Czerwinski, E. Borowski, Biochem. Pharmacol. 37 (1988) 827–836.
[35] C.M. Gary-Bobo, Biochimie 71 (1989) 37–47.
[36] A.W. Hing, S.P. Adams, D.F. Silbert, R.E. Norberg, Biochemistry 29 (1990) 4144–4156.
[37] M.H. Levitt, D. Suter, R.R. Ernst, J. Chem. Phys. 80 (1984) 3064–3068.
[38] Y. Harada, Y. Iitaka, Acta Cryst. B30 (1974) 1452–1459.
[39] L. Pauling, R.B. Corey, H.R. Branson, Proc. Natl. Acad. Sci. USA 37 (1951) 205–211.
[40] L. Falkowski, A. Jarzebski, B. Stefanska, E. Bylec, E. Borowski, J. Antibiot. 33 (1980) 103–104.
[41] A. Czerwinski, T. Zieniawa, E. Borowski, L.G. Micossi, J. Antibiot. 43 (1990) 680–683.
[42] J. Grzybowska, E. Borowski, J. Antibiot. 43 (1990) 907–908.
[43] J. Seelig, Biochim. Biophys. Acta 515 (1978) 105–140.
[44] V. Luzzati, Biol. Membr. 1 (1968) 71–123.
[45] M.J. Janiak, D.M. Small, G.G. Shipley, Biochemistry 15 (1976) 4575–4580.
[46] J. Seelig, Q. Rev. Biophys. 10 (1977) 353–418.
[47] A.C. McLaughlin, P.R. Cullis, M.A. Hemminga, D.I. Hoult, G.K. Radda, G.A. Ritchie, P.J. Seeley, R.E. Richards, FEBS Lett. 57 (1975) 213–218.
[48] P.R. Cullis, B. de Kruyff, R.E. Richards, Biochim. Biophys. Acta 426 (1976) 433–446.
[49] S.J. Kohler, M.P. Klein, Biochemistry 16 (1977) 519–526.
[50] M.F. Brown, J. Seelig, Biochemistry 17 (1978) 381–384.
[51] M.A. Hemminga, P.R. Cullis, J. Magnet. Reson. 47 (1982) 307–323.
[52] M.R. Vist, J.H. Davis, Biochemistry 29 (1990) 451–464.
[53] T.P.W. McMullen, R.N.A.H. Lewis, R.N. McElhaney, Biochemistry 32 (1993) 516–522.